Published in final edited form as:
Arthritis Rheum. 2013 August ; 65(8): 2048–2058. doi:10.1002/art.37987.

MRI-based three-dimensional bone shape of the knee predicts onset of knee osteoarthritis: Data from the Osteoarthritis Initiative

Tuhina Neogi[1], **Michael Bowes**[2], **Jingbo Niu**[1], **Kevin De Souza**[2], **Graham Vincent**[2], **Joyce Goggins**[1], **Yuqing Zhang**[1], and **David T. Felson**[1,3]

[1]Clinical Epidemiology Research and Training Unit, Boston University School of Medicine, Boston, MA

[2]Imorphics, Manchester, UK

[3]Arthritis Research UK Epidemiology Unit, University of Manchester, Manchester, UK

Abstract

Objective—To examine whether MRI-based 3D bone shape predicts the onset of radiographic knee osteoarthritis (OA).

Methods—We conducted a case-control study within the Osteoarthritis Initiative by identifying knees that developed incident tibiofemoral radiographic knee OA (case knees) over follow-up, and matching them to two random control knees. Using knee MRI's, we used active appearance modeling of the femur, tibia and patella and linear discriminant analysis to identify vectors that best classified knees having OA vs. not. Vectors were scaled such that -1 and +1 represented the mean non-OA and mean OA shapes, respectively. We examined the relation of 3D bone shape to incident OA (new onset Kellgren and Lawrence (KL) grade ≥2) occurring 12 months later using conditional logistic regression.

Results—178 case knees (incident OA) were matched to 353 control knees. The whole joint (i.e., tibia, femur, and patella) 3D bone shape vector had the strongest magnitude of effect, with knees in the highest tertile having 3.0 times higher likelihood of developing incident radiographic knee OA 12 months later compared with those in the lowest tertile (95% CI 1.8-5.0, p<0.0001). The associations were even stronger among knees that showed completely normal radiographs before incidence (KL grade 0) (OR 12.5, 95% CI 4.0-39.3). Bone shape at baseline, often several years before incidence, predicted later OA.

Conclusions—MRI-based 3D bone shape predicted the later onset of radiographic OA. Further study is warranted to determine whether such methods can detect treatment effects in trials and provide pathophysiologic insight into OA development.

Introduction

Knee osteoarthritis (OA) is a leading cause of disability among US older adults,[1] with the burden rising in part due to aging of the population and increasing obesity.[2] There are presently no therapies available to prevent OA or its progression. The current standard of using knee x-rays to identify OA onset or joint-space width to monitor progression is likely

Contact information: T. Neogi, 650 Albany St., Clin Epi Unit, Suite X200, Boston, MA, USA, 02118; Tel: 617-638-5180; Fax: 617-638-5239; tneogi@bu.edu.

Disclosures
The other authors have no potential financial conflicts of interest to declare.

not sensitive enough to accurately assess the effects of potentially promising treatments. As examples, the risedronate[3] and oral iNOS inhibitor[4] trials did not meet their primary end-points based upon radiographic joint-space narrowing despite supportive preliminary data, raising concerns about insensitivity of radiography. Thus, there is a compelling need to develop improved imaging biomarkers for OA to enable development and testing of treatments. Such imaging biomarkers would also help identify persons at risk for developing knee OA and/or rapid disease progression, permitting the study of pertinent risk factors and targeted enrollment into trials.

Because knee OA is thought to be largely a mechanically-driven process,[5] a promising target for an OA imaging biomarker may be to exploit the ability of bone to adapt to mechanical influences.[6] In particular, bone can readily change its shape in response to stresses acting upon it (Wolff's Law),[6,7] suggesting that such alterations may be feasibly assessed in a practical time-frame, making it attractive as a potential imaging end-point for trials. Additionally, subtle differences in bone shape or geometry itself could lead to abnormal joint loading and predispose to OA.

Lending support to the importance of bone shape to OA, abnormalities such as congenital hip dysplasia and femoracetabular impingement as well as more subtle femoracetabular shape differences identified through morphometric measurements or statistical modeling have been associated with hip OA.[8-11] Although the geometry of the knee may be more complex than that of the hip, differences in knee joint shape between ethnic groups have been identified.[12] Tibiofemoral joint shape alterations on radiographs have been associated with prevalent knee OA cross-sectionally.[13] However, some of the changes identified may have been related to position during image acquisition, and more generally, radiographs do not permit visualization of three-dimensional (3D) bone shape changes.

While MRI studies have described increased tibial plateau size and alterations of the bony surface contour (*e.g.*, subchondral bone attrition), even at the pre-radiographic OA stage,[14-16] those findings do not fully capture the spectrum and complexity of the 3D bone shape changes that occur in OA. More recently, a small cross-sectional study of 24 knees used MR images to evaluate the variability in knee articular surface geometry using statistical shape modeling to compare those with and without OA.[17]

With increased availability and use of MRI, 3D bone shape changes related to knee OA can now be more readily characterized on a larger scale using more advanced statistical modeling methods to detect subtle shape variations for improved sensitivity. We examined the ability of 3D bone shape to predict the incidence of knee OA at least 12-months prior to its onset using data from the Osteoarthritis Initiative (OAI).

Methods

Study Sample

We used publicly available data from the OAI, which is a longitudinal observational cohort study aiming to study the natural history of and risk factors for knee OA. Subjects with or at high risk of knee OA aged 45-79 were recruited from 4 clinical centers across the US. Details of the cohort have been published elsewhere[18] and can be found at the OAI website: http://oai.epi-ucsf.org/datarelease/StudyOverview.asp

Imaging

Knee Radiography—Participants underwent bilateral posteroanterior fixed flexion weight-bearing knee radiographs at baseline and annually.[19] In this study, we used the centrally-adjudicated radiographic reading data from baseline to the 48-month clinic visit,

inclusively. Radiographs were read by an academically-based radiologist and two rheumatologists in a panel of three, with disagreement resolved by adjudication.[20] Incident tibiofemoral radiographic knee OA was defined as new onset Kellgren and Lawrence (KL) grade ≥2 identified in a follow-up study visit (i.e., 12, 24, 36, or 48-month study visits) among knees that were KL<2 at baseline; as per the OAI central readings, new onset osteophytes with no narrowing were not considered as incident OA.[21] Incident knee OA could include incident medial or lateral tibiofemoral OA.

Magnetic Resonance Imaging (MRI)—Participants underwent bilateral knee MRI (3.0T, Siemens Trio) at baseline and annually. We used the sagittal 3D double echo steady state with water excitation (DESS-we) sequence for determination of the 3D bone shape.

Statistical Modeling of 3D Bone Shape

Below we outline the two *independent* training sets used to develop the model employed in our analyses of a third independent test set.

We used an independent training set of 96 knees to train models used for automatic segmentation, using active appearance models (AAMs). AAMs are a form of statistical shape modeling method that learns the variation in shape and gray-scale texture ('appearance') of objects from a training set (such as the bones from an MRI), and encodes shape and appearance as principal components.[22,23] AAMs for the femur, tibia and patella were built using custom software based on published AAM methodology[22] (Imorphics, Manchester, UK) from 96 examples chosen so as to contain approximately equal numbers of knees from each KL grade. All models within this study were generated so as to account for 98% of variance in the shape data from the training set. During the model building process, principal components are added until this figure is reached. This resulted in 69 principal components for the femur shape, 66 for the tibia, and 59 for the patella. Once trained, AAMs can automatically segment bones in MR images by matching principal components of shape and appearance using the least squares sum of residuals. As a consequence of this process, each time a new image is searched, the distance along each of the principal components for the object is recorded. This has the effect of reducing shape dimensionality; in the case of the femur, this reduces a triangulated mesh of over 100,000 points to 69 floating point values, one for each principal component in the model. The accuracy of the segmentations for the knee has been validated.[24,25]

For our particular models, accuracy of the automated segmentations was further assessed using test-retest MRIs of 19 participants (38 images) with none-to-moderate degrees of clinical OA, prepared as a pilot study for OAI, using the same MR sequence.[26] The bone surface was manually segmented as previously described.[27] Mean point-to-surface distances were calculated between the manual and automated segmentations. Mean point-to-surface errors were as follows: femur, 0.49mm; tibia, 0.53mm; patella, 0.57mm; *i.e.,* approximately the size of one voxel.

We used a second independent training set to identify vectors within this shape space that could discriminate between distinct groups (*e.g.,* OA and non-OA) using linear discriminant analysis (LDA), a form of supervised learning.[28,29] LDA is used in pattern recognition and machine learning to find features that differentiate objects into separate groups,[30] such as used in medical imaging (*e.g.,* neuroimaging) and facial recognition.[31,32] LDA identifies the line in multi-dimensional space that best separates 2 groups. This further reduces the shape dimensionality to a single scalar value, being the distance along the LDA vector for each bone or combination of bones. We used a total of 607 knees (one knee/person) from OAI (296 with KL=0 or 1; 311 with KL=2-4, median KL=3) (independent of the training set used to develop the AAM) to train the LDA vectors. The 607 images were searched using these

AAMs, and the values for the principal components recorded for each of the femur, tibia and patella bones. The point sets of the femur and tibia were combined and a shape model built for the combined femur and tibia shape. A combined model of femur, tibia and patella was also constructed. LDA was performed with the principal components for each bone as inputs, with each example labeled as OA or non-OA. The distribution of the femur shapes in the training set is shown in **Figure 1** using a Sammon plot, a non-linear dimension reduction that displays the 607 results in 2 dimensions while preserving the distances between examples as far as possible.[33]

New bone shapes (*e.g.*, those generated by an AAM search of the case-control study sample for this study) can be expressed as principal components, which in turn are projected onto the LDA vector, and recording the distance along the vector. Distance along the vector was normalized by treating the mean non-OA shape as -1 and the mean OA shape as +1. Reproducibility of the method was tested in a separate set of 35 OA knees that were imaged one week apart, using the same OAI image acquisition sequence at a single OAI site.[27] Reproducibility of the method was good, with SDD (95% confidence limits on a Bland-Altman plot) being 0.3 normalized units for the whole joint model.

Visualization of changes in population shape

Extreme examples of OA and non-OA shape were created by finding the points at -3SD of the OA and +3SD of the non-OA groups, on a line passing through the means of the OA and non-OA groups (**Figure 1**) and were examined using a 3D viewer (Imorphics, Manchester, UK).

Statistical Analyses

We conducted a matched case-control study. Each knee that was identified as having developed incident tibiofemoral radiographic knee OA (case) was matched to two randomly selected control knees that remained free of tibiofemoral OA at that same clinic visit (index visit) as when the case knee developed incident OA, matched by baseline KL grade. We shall label this incident knee OA even though the absence of radiographic image assessment of the patellofemoral joint prohibits our evaluation of incidence there. We included in our study sample all knees that developed incident knee OA at any time during follow-up as well as their matched control knees. For individuals in whom both knees could be selected for this study, we randomly selected a single knee from such individuals (n=25).

We evaluated five 3D bone shape vectors as predictors of incidence: each bone separately (femur, tibia, patella), femur and tibia together (tibiofemoral), and whole joint (femur, tibia, patella) combined. We first examined the relation of these 3D whole bone shape vectors 12 months prior to the index visit to the risk of incident radiographic knee OA (*i.e.*, occurring 12 months later) using conditional logistic regression. That is, we used 3D bone shape data from the clinic visit 12-months prior to the occurrence of incident radiographic knee OA (or the index visit for the control knees). We repeated these analyses limited to those case and control knees that were KL=0 at baseline to reduce the likelihood that changes of early OA (at KL=1) were reflected in the 3D bone shape. We also examined the relation of the OAI's baseline study visit 3D bone shape (*i.e.*, irrespective of time of later incident disease) to the occurrence of incident radiographic knee OA at any time during OAI's follow-up visits. We finally evaluated the relationship of 3D bone shape to incident radiographic knee OA occurring concurrently (*i.e.*, 3D bone shape vector from the *same* visit that incident radiographic knee OA occurred) to confirm our prior findings that bone shape was related to concurrent OA.

The 3D bone shape vectors were assessed as continuous variables as well as categorized into tertiles, with the highest tertile containing values closer to the mean OA shape, while the lowest tertile contains values closer to the mean non-OA shape. Analyses were adjusted for age, sex, BMI.

Results

Among knees that were free of radiographic OA at baseline in OAI, 178 knees developed incident radiographic knee OA during the follow-up; these were matched to 353 knees. As can be seen in **Table 1**, the average age of the cases and controls was 61 years; the majority were female and White; and, as expected, the BMI was slightly higher in cases than controls.

The mean 3D bone shape vectors increased (*i.e.*, became more “OA”-like) from baseline to the 12-month visit prior to incident radiographic knee OA and to the visit at which incident radiographic knee OA was identified among case knees, while the 3D bone shape vectors remained stable for the control knees over these three time-points (**Table 1**). For example, for the whole joint 3D bone shape vector, which incorporated the femur, tibia, and patella, the mean values for the case knees were -0.32 at baseline, -0.23 at the 12-month visit prior to incident radiographic knee OA, and -0.01 at the incident radiographic knee OA visit, whereas the corresponding values were -0.52, -0.51, -0.44 for the control knees.

Each of the five 3D bone shape vectors 12 months prior to the index visit was significantly associated with incident radiographic knee OA (**Table 2**). The 3D bone shape vector that included the whole joint (*i.e.*, all 3 bones) had the strongest magnitude of effect, with those knees in the highest tertile having 3 times higher likelihood of developing incident radiographic knee OA 12 months later compared with those in the lowest tertile (95% CI 1.8-5.0, $p<0.0001$). There was also a dose-response relationship between the whole joint 3D bone shape vector and risk of incident radiographic knee OA ($p<0.0001$) when assessed as tertiles as well as a continuous vector. Each standard deviation unit change (towards the mean OA shape) was associated with 68% higher risk of incident radiographic knee OA (95% CI 1.4-2.1, $p<0.0001$) (**Table 2**). The 3D bone shape vector of the femur alone had the largest effect among each of the individual bone vectors, with those in the highest tertile having 2.7 times higher chance than those in the lowest tertile of developing incident radiographic knee OA 12 months later (95% CI 1.7-4.5, $p<0.0001$). Of note, adjustment for the important potential confounders did not appreciably alter the effect estimates from the crude estimates, suggesting the associations noted are not substantially influenced by age, sex, or BMI (see **Table 2**).

Because KL=1 knees may have early changes of OA that could be reflected in the 3D bone shape, we repeated the above analyses limited to those knees that were KL=0 at baseline (n=46).These knees were matched to 92 randomly selected control knees that were also KL=0 at baseline. In these analyses, despite smaller numbers limiting precision, strong relationships were noted (**Table 3**, first results column). For example, knees in the highest tertile of the whole joint vector 12 months prior to the index visit were 12.5 times more likely to develop incident radiographic knee OA than knees in the lowest tertile (95% CI 4.0-39.3, $p<0.0001$). Again, the femur 3D bone shape vector performed the best out of the three individual bone vectors (OR 6.5 for highest versus lowest tertile, 95% CI 2.3-18.3, $p=0.0004$). All 3D bone shape vectors were significantly associated with incident radiographic knee OA among these knees with KL=0 at baseline.

Because knee OA onset can occur at any time after a baseline study visit, we assessed the ability of 3D bone shape from the baseline visit to predict the later occurrence of incident

knee OA, irrespective of timing of OA onset. In these analyses, the median time from the OAI baseline visit to the study visit at which incident OA was identified was 24 months. As can be seen in **Table 4** (first results column), the magnitudes of effect were similar to those obtained with 3D bone shape 12 months prior to the onset of radiographic knee OA (in **Table 2**), suggesting that the vector can robustly discriminate between knees that will develop OA in the future (*i.e.*, 12, 24, 36, or 48 months later) from those that will not. That is, once a certain shape is present (*i.e.*, at baseline), there is a high likelihood of developing OA at some point in the future, even years later. When we further excluded the case knees that developed incident OA at 12-months (N=82) (and their matched controls) to ensure that this group did not unduly influence these results, the magnitudes of effect remained similar. For example, for the knees in the highest tertile of the whole joint vector, the OR was 3.0 (95% CI 1.5-6.0, p=0.002) when knees with incident OA at 12-months were excluded, compared with an OR of 2.5 (95% CI 1.5-4.1, p=0.0004) for the whole sample (**Table 4**, second results column compared with first results column). Larger effect estimates were also noted for knees that were KL=0 at baseline in terms of predicting OA onset at any one of the later time-points as well as when knees with incident OA at 12-months were excluded (*e.g.*, whole joint vector OR=6.2, p=0.001 and OR=6.6, p=0.005 for highest vs. lowest tertile, respectively) (**Table 4**, third and fourth results column). This indicates that 3D bone shape from the baseline visit could discriminate which groups of knees were highly likely to develop OA 24-48 months later, even among KL=0 knees (**Table 4**, second and fourth results column).

When we examined bone shape at the same study visit as that of OA incidence, the relation of bone shape and OA was strong, confirming prior findings (**Table 3**, second results column). Similar to the findings above, the whole joint 3D bone shape vector had the strongest relationship to incident radiographic knee OA, and the femur had the strongest relationship among each of the individual bones.

Figure 2 depicts examples of the OA and non-OA shapes for the population within the LDA training set representing “A” and “B” in **Figure 1**. Differences in femur shape between OA and non-OA shapes include a general widening and flattening of the condyles on the medial side, and an increased ridge of ‘osteophytic’ growth around all of the cartilage plate, along with a narrowing of the notch. Differences in tibial shape include a corresponding widening and flattening of the condyles, and an increased ridge of ‘osteophytic’ growth around all of cartilage plates, with the tibial spines moving closer together. The patella also has an increased size of cartilage plate, accompanied by an osteophytic ridge.

Discussion

This is the first large-scale study of 3D shape vectors to identify an imaging-based biomarker in knees free of radiographic tibiofemoral OA at baseline. This also represents the first effort to examine whole joint bone shape (comprising 3D bone shapes of the femur, tibia, and patella) as a predictor of subsequent disease development. Importantly, this study is the first to report not just the properties of a statistical shape model containing OA examples, but confirms that the measures are useful with an independent test set. We have demonstrated that 3D vectors, trained on OA and non-OA shapes, can identify knees without OA that are at risk of developing OA 12 months later and beyond, and that position along this vector is associated with OA incidence.

That bone can change dynamically to such an extent that it is measurable during the course of disease is not surprising. Subchondral bone in OA has increased thickness and volume, leading to alterations in apparent and material bone density.[34-38] Alterations in trabecular bone structure in knee OA have also been identified.[39-42] In the high bone turnover state of

OA, which can be detected by scintigraphy,[43] mineral deposition may be attenuated, leading to relative hypomineralization and weaker bone that is more easily deformed.[37,44] Other well-known changes in bone shape in knee OA include osteophyte formation and growth, hallmarks of OA, increased tibial plateau size, and alterations of the bony surface contour (subchondral bone attrition).[14-16] Changes in the intercondylar notch has also been previously noted,[45,46] but the whole 3D shape has not been described before, nor the relative scale of the change. Our work confirms and extends these previous observations.

Importantly, the normal functioning of diarthrodial joints depends on stability and appropriate distribution of load across the joint surfaces, which in turn is dependent upon the geometry and material properties of the articulating joint tissues. Thus, the relation of bone shape to OA development should be expected given that alterations in joint geometry affect joint congruity and can lead to maldistribution of load.[47] Some bone shape changes may have adverse consequences for overlying cartilage. It has been hypothesized that cartilage loss is a mechanically-mediated process that is more likely to occur in regions subjected to high stress; such areas of high stress are likely to be influenced by bone shape.[25]

While we demonstrated in this study that bone shape changes precede the onset of radiographic OA by at least a year and longer, that latter event may be late in disease development. It is not clear how long some evidence of disease is present before it is apparent on the radiograph. However, two findings from our study may suggest that bone shape changes very early in the disease process, or perhaps may even be an inherent trait: 1) That knees with grade 0 radiographs and abnormal bone shapes were highly likely to develop OA; and 2) That bone shape even two to four years before radiographic OA incidence denoted an increased risk of disease (*i.e.*, baseline bone shape irrespective of timing of later OA incidence). It is also possible that bone shape is an inherited factor that influences disease development and then changes further with the disease process. The ultimate relation of bone shape to disease awaits other longitudinal studies.

Much of the 3D bone shape identified within this study is unlikely to be accurately or well-visualized on standard planar radiographs, particularly due to issues with projection, rotation and resolution. A good example of this is that the growth of a distinctive ridge around the femoral plate appears in a radiograph as a small bony spur, and seems almost inconsequential. Changes in the bone such as flattening, widening and ridge formation are difficult to quantify in radiograph studies, and are therefore not typically studied.

In addition to having analytic advantages as an imaging biomarker, many of these bone changes have implications for understanding the OA pathophysiology and where the biomechanical stresses may be acting. For example, the widening and flattening of the bone structures is certain to change the distribution of mechanical load on the joint, presumably creating further change in bone. It also becomes apparent that alignment as well as the “joint-space”, which is thought to comprise cartilage and meniscus, are also influenced by bone shape; as OA progresses, some articular areas have bone laid down, while others appear to have bone “taken away”. Osteophytes which are generally described as discrete lesions on radiographs and morphologic assessments of MRI can be seen to actually be a ridge-like laying down of bone circumferentially around the entire articular surface. This ridge may cause mechanical damage to other structures such as the meniscus and overlying cartilage.

Previous studies that have examined the relationship of 2D shape to OA[8,9,13] faced limitations of using manual markup from anteroposterior radiographs, including inability to discern projection effects or rotation from true shape differences, and inability to capture most of the 3D shape changes (*e.g.*, the patellofemoral joint and the osteophytic ridge).

These are particularly difficult challenges for knee radiographs. An advantage to using MRI over radiographs to examine bone shape is obviously the 3D nature of the data. MRI's also avoid difficulties in interpreting findings that may be related to positioning during image acquisition and projection effects.

One prior small cross-sectional study has used MRI to assess differences in the principal components of the tibia and femur geometry assessed by MRI between the Control and disease groups selected from the OAI using statistical shape modeling.[17] However, in this study and other prior approaches, an independent test set was not used to validate the findings, which is necessary as it is highly likely when training a shape model that some principal components will spuriously correlate with any labeling of the examples in the model (*e.g.*, OA vs. non-OA). In our study, we used independent training sets at each stage, thereby reducing the possibility of false positive associations.

Another difference is our approach to analyzing the principal components derived from statistical modeling. Prior applications based on radiographs have analyzed individual principal components (or modes) to identify which one is the most discriminant,[8,9,13,17] meaning that the data from the remaining principal components are not used. Our approach using LDA to identify a single vector takes into account information from all of the principal components that account for 98% of the variation, providing greater insight into correlated shape changes.

While our findings certainly point to the promise of such imaging and statistical methods for prediction of knee OA onset and changes, certain limitations should be acknowledged. First, our methods required the assumption that shape change is linear. The model demonstrates that at least part of the change in OA is linear and systematic, although there may be other important effects which are non-linear, or which occur only in subsets of individuals. Non-linear approaches may be even more discriminating. Second, we modeled the shape change of whole bones, but local regional changes may be more sensitive and insightful; this will be incorporated in future work. Third, a number of factors are likely to contribute to bone shape changes, including gender, race, BMI, alignment, and mechanical damage to the ligaments. Nonetheless, OA-related shape changes could be identified despite other contributors to change in shape. Fourth, early changes may not be the same as late changes, and therefore study of the full spectrum of OA development and progression is necessary.

In summary, we have demonstrated MRI-based 3D bone shape to be associated with development of incident radiographic knee OA, including that occurring one year later and beyond. The patterns of change provide opportunities to gain further insight into biomechanical and other pathophysiologic influences in OA pathogenesis. Use of AAM to comprehensively quantify MRI-based 3D bone shape of the knee joint has potential as an imaging biomarker and warrants further study as an imaging endpoint in clinical trials.

Acknowledgments

Funding:

NIH AR47785, NIH AR051568, NIH AR055127, Arthritis Foundation Arthritis Investigator Award

The OAI is a public-private partnership comprised of five contracts (N01-AR-2-2258; N01-AR-2-2259; N01-AR-2-2260; N01-AR-2-2261; N01-AR-2-2262) funded by the National Institutes of Health, a branch of the Department of Health and Human Services, and conducted by the OAI Study Investigators. Private funding partners include Merck Research Laboratories; Novartis Pharmaceuticals Corporation, GlaxoSmithKline; and Pfizer, Inc. Private sector funding for the OAI is managed by the Foundation for the National Institutes of Health.

Michael Bowes, Kevin De Souza and Graham Vincent are employees and shareholders of Imorphics Ltd.

References

1. Guccione AA, Felson DT, Anderson JJ, et al. The effects of specific medical conditions on the functional limitations of elders in the Framingham Study. Am. J. Public Health. Mar; 1994 84(3): 351–358. [PubMed: 8129049]
2. Nguyen US, Zhang Y, Zhu Y, Niu J, Zhang B, Felson DT. Increasing prevalence of knee pain and symptomatic knee osteoarthritis: survey and cohort data. Ann. Intern. Med. Dec 6; 2011 155(11): 725–732. [PubMed: 22147711]
3. Bingham CO 3rd, Buckland-Wright JC, Garnero P, et al. Risedronate decreases biochemical markers of cartilage degradation but does not decrease symptoms or slow radiographic progression in patients with medial compartment osteoarthritis of the knee: results of the two-year multinational knee osteoarthritis structural arthritis study. Arthritis Rheum. Nov; 2006 54(11):3494–3507. [PubMed: 17075851]
4. Hellio Le Graverand-Gastineau MP, Clemmer R, Redifer P, et al. A 2-year randomized, double-blind, placebo-controlled, multicenter study of an oral selective iNOS inhibitor in subjects with symptomatic osteoarthritis of the knee. Osteoarthritis Cartilage. 2012; 20(Suppl 1):S38.
5. Felson DT, Lawrence RC, Dieppe PA, et al. Osteoarthritis: new insights. Part 1: the disease and its risk factors. Ann. Intern. Med. Oct 17; 2000 133(8):635–646. [PubMed: 11033593]
6. Goldring SR. The role of bone in osteoarthritis pathogenesis. Rheum. Dis. Clin. North Am. Aug; 2008 34(3):561–571. [PubMed: 18687272]
7. Chen JH, Liu C, You L, Simmons CA. Boning up on Wolff's Law: mechanical regulation of the cells that make and maintain bone. J. Biomech. Jan 5; 2010 43(1):108–118. [PubMed: 19818443]
8. Gregory JS, Waarsing JH, Day J, et al. Early identification of radiographic osteoarthritis of the hip using an active shape model to quantify changes in bone morphometric features: can hip shape tell us anything about the progression of osteoarthritis? Arthritis Rheum. Nov; 2007 56(11):3634–3643. [PubMed: 17968890]
9. Lynch JA, Parimi N, Chaganti RK, Nevitt MC, Lane NE. The association of proximal femoral shape and incident radiographic hip OA in elderly women. Osteoarthritis Cartilage. Oct; 2009 17(10): 1313–1318. [PubMed: 19427402]
10. Baker-LePain JC, Lane NE. Relationship between joint shape and the development of osteoarthritis. Curr. Opin. Rheumatol. Sep; 2010 22(5):538–543. [PubMed: 20644480]
11. Dudda M, Kim YJ, Zhang Y, et al. Morphologic differences between the hips of Chinese women and white women: could they account for the ethnic difference in the prevalence of hip osteoarthritis? Arthritis Rheum. Oct; 2011 63(10):2992–2999. [PubMed: 21647861]
12. Mahfouz M, Abdel Fatah EE, Bowers LS, Scuderi G. Three-dimensional morphology of the knee reveals ethnic differences. Clin Orthop Relat Res. Jan; 2012 470(1):172–185. [PubMed: 21948324]
13. Haverkamp DJ, Schiphof D, Bierma-Zeinstra SM, Weinans H, Waarsing JH. Variation in joint shape of osteoarthritic knees. Arthritis Rheum. Nov; 2011 63(11):3401–3407. [PubMed: 21811994]
14. Ding C, Cicuttini F, Scott F, Cooley H, Boon C, Jones G. Natural history of knee cartilage defects and factors affecting change. Arch. Intern. Med. Mar 27; 2006 166(6):651–658. [PubMed: 16567605]
15. Dore D, Quinn S, Ding C, Winzenberg T, Cicuttini F, Jones G. Subchondral bone and cartilage damage: a prospective study in older adults. Arthritis Rheum. Jul; 2010 62(7):1967–1973. [PubMed: 20506256]
16. Reichenbach S, Guermazi A, Niu J, et al. Prevalence of bone attrition on knee radiographs and MRI in a community-based cohort. Osteoarthritis Cartilage. Sep; 2008 16(9):1005–1010. [PubMed: 18367415]
17. Bredbenner TL, Eliason TD, Potter RS, Mason RL, Havill LM, Nicolella DP. Statistical shape modeling describes variation in tibia and femur surface geometry between Control and Incidence groups from the osteoarthritis initiative database. J. Biomech. Jun 18; 2010 43(9):1780–1786. [PubMed: 20227696]

18. Lester G. Clinical research in OA--the NIH Osteoarthritis Initiative. J Musculoskelet Neuronal Interact. Oct-Dec;2008 8(4):313–314. [PubMed: 19147953]
19. Peterfy C, Li J, Zaim S, et al. Comparison of fixed-flexion positioning with fluoroscopic semi-flexed positioning for quantifying radiographic joint-space width in the knee: test-retest reproducibility. Skeletal Radiol. Mar; 2003 32(3):128–132. [PubMed: 12605275]
20. Felson DT, Nevitt MC, Yang M, et al. A new approach yields high rates of radiographic progression in knee osteoarthritis. J. Rheumatol. Oct; 2008 35(10):2047–2054. [PubMed: 18793000]
21. Felson DT, Niu J, Guermazi A, Sack B, Aliabadi P. Defining radiographic incidence and progression of knee osteoarthritis: suggested modifications of the Kellgren and Lawrence scale. Ann. Rheum. Dis. Nov; 2011 70(11):1884–1886. [PubMed: 21908453]
22. Cootes TF, Edwards GJ, Taylor CJ. Active appearance models. IEEE Trans Pattern Anal Mach Intell. 2001; 23(6):681–685.
23. Williams TG, Holmes AP, Bowes M, et al. Measurement and visualisation of focal cartilage thickness change by MRI in a study of knee osteoarthritis using a novel image analysis tool. Br. J. Radiol. Nov; 2010 83(995):940–948. [PubMed: 20223905]
24. Solloway S, Hutchinson CE, Waterton JC, Taylor CJ. The use of active shape models for making thickness measurements of articular cartilage from MR images. Magn. Reson. Med. Jun; 1997 37(6):943–952. [PubMed: 9178247]
25. Williams, TG.; Vincent, G.; Bowes, M., et al. Automatic segmentation of bones and inter-image anatomical correspondence by volumetric statistical modeling of knee MRI.. Paper presented at: Proceedings of the 2010 IEEE International Conference on Biomedical Imaging: From nano to macro2010; Rotterdam, Netherlands.
26. Eckstein F, Hudelmaier M, Wirth W, et al. Double echo steady state magnetic resonance imaging of knee articular cartilage at 3 Tesla: a pilot study for the Osteoarthritis Initiative. Ann. Rheum. Dis. Apr; 2006 65(4):433–441. [PubMed: 16126797]
27. Hunter DJ, Bowes MA, Eaton CB, et al. Can cartilage loss be detected in knee osteoarthritis (OA) patients with 3-6 months' observation using advanced image analysis of 3T MRI? Osteoarthritis Cartilage. May; 2010 18(5):677–683. [PubMed: 20219688]
28. Cootes TF, Cooper D, Taylor CJ, Graham J. Active shape models - their training and application. Computer Vision and Image Understanding. 1995; 61(1):38–59.
29. Cootes TF, Twining CJ, Petrovic V, Shchestowitz R, Taylor CJ. Groupwise construction of appearance models using piece-wise affine deformations. Proceedings British Machine Vision Conference. 2005; 2(879-888)
30. Fisher FA. The use of multiple measurements in taxonomic problems. Annals of Eugenics. 1936; 7:179–188.
31. Davies RH, Twining CJ, Allen PD, Cootes TF, Taylor CJ. Shape discrimination in the hippocampus using an MDL model. Inf Process Med Imaging. Jul.2003 18:38–50. [PubMed: 15344445]
32. Martinez AM, Kak AC. PCA versus LDA. IEEE Trans Pattern Anal Mach Intell. 2001; 23(2):228–233.
33. Sammon JW Jr. A nonlinear mapping for data structure analysis. IEEE Transactions on Computers. 1969; C-18(5):401–409.
34. Buckland-Wright C. Subchondral bone changes in hand and knee osteoarthritis detected by radiography. Osteoarthritis Cartilage. 2004; 12(Suppl A):S10–19. [PubMed: 14698636]
35. Radin EL, Rose RM. Role of subchondral bone in the initiation and progression of cartilage damage. Clin Orthop Relat Res. Dec.1986 (213):34–40. [PubMed: 3780104]
36. Grynpas MD, Alpert B, Katz I, Lieberman I, Pritzker KP. Subchondral bone in osteoarthritis. Calcif. Tissue Int. Jul; 1991 49(1):20–26. [PubMed: 1893292]
37. Li B, Aspden RM. Mechanical and material properties of the subchondral bone plate from the femoral head of patients with osteoarthritis or osteoporosis. Ann. Rheum. Dis. Apr; 1997 56(4): 247–254. [PubMed: 9165997]

38. Li B, Aspden RM. Composition and mechanical properties of cancellous bone from the femoral head of patients with osteoporosis or osteoarthritis. J. Bone Miner. Res. Apr; 1997 12(4):641–651. [PubMed: 9101376]
39. Patel V, Issever AS, Burghardt A, Laib A, Ries M, Majumdar S. MicroCT evaluation of normal and osteoarthritic bone structure in human knee specimens. J. Orthop. Res. Jan; 2003 21(1):6–13. [PubMed: 12507574]
40. Messent EA, Buckland-Wright JC, Blake GM. Fractal analysis of trabecular bone in knee osteoarthritis (OA) is a more sensitive marker of disease status than bone mineral density (BMD). Calcif. Tissue Int. Jun; 2005 76(6):419–425. [PubMed: 15834503]
41. Woloszynski T, Podsiadlo P, Stachowiak GW, Kurzynski M, Lohmander LS, Englund M. Prediction of progression of radiographic knee osteoarthritis using tibial trabecular bone texture. Arthritis Rheum. Mar; 2012 64(3):688–695. [PubMed: 21989629]
42. Kraus VB, Feng S, Wang S, et al. Trabecular morphometry by fractal signature analysis is a novel marker of osteoarthritis progression. Arthritis Rheum. Dec; 2009 60(12):3711–3722. [PubMed: 19950282]
43. Dieppe P, Cushnaghan J, Young P, Kirwan J. Prediction of the progression of joint space narrowing in osteoarthritis of the knee by bone scintigraphy. Ann. Rheum. Dis. Aug; 1993 52(8): 557–563. [PubMed: 8215615]
44. Day JS, Ding M, van der Linden JC, Hvid I, Sumner DR, Weinans H. A decreased subchondral trabecular bone tissue elastic modulus is associated with pre-arthritic cartilage damage. J. Orthop. Res. Sep; 2001 19(5):914–918. [PubMed: 11562141]
45. Shepstone L, Rogers J, Kirwan JR, Silverman BW. Shape of the intercondylar notch of the human femur: a comparison of osteoarthritic and non-osteoarthritic bones from a skeletal sample. Ann. Rheum. Dis. Oct; 2001 60(10):968–973. [PubMed: 11557655]
46. Wada M, Tatsuo H, Baba H, Asamoto K, Nojyo Y. Femoral intercondylar notch measurements in osteoarthritic knees. Rheumatology (Oxford). Jun; 1999 38(6):554–558. [PubMed: 10402077]
47. Bullough PG. The geometry of diarthrodial joints, its physiologic maintenance, and the possible significance of age-related changes in geometry-to-load distribution and the development of osteoarthritis. Clin Orthop Relat Res. May.1981 (156):61–66. [PubMed: 7226665]

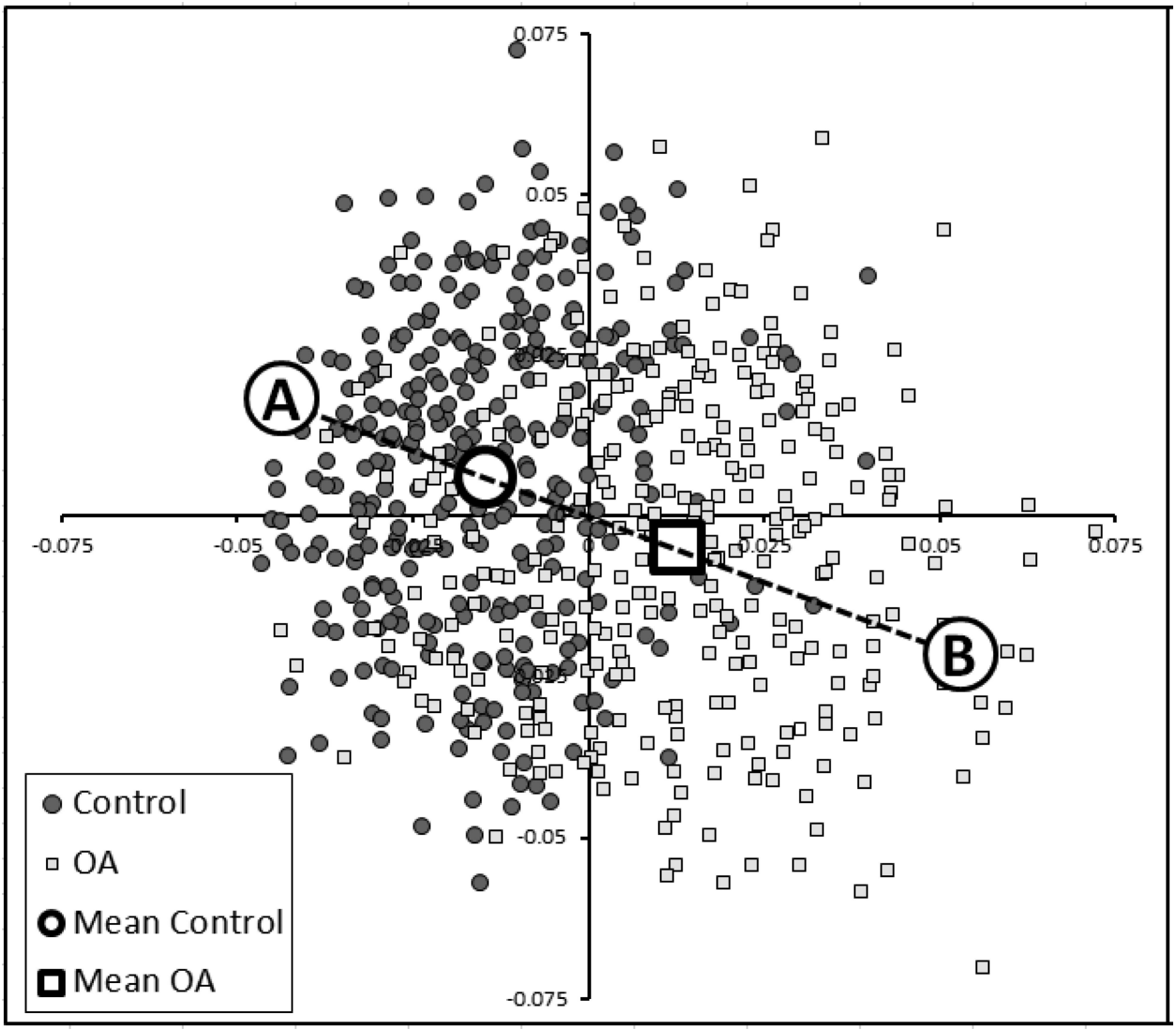

Figure 1.

Sammon plots illustrating the shape distributions of the 607 femurs used in the training set. LDA was used to determine the best single vector that discriminated the two groups (*e.g.*, non-OA ("A") vs. OA ("B")). Each individual femur's results is encoded as 70 principal components, creating a 70-dimensional value. The Sammon plot reduces these 70 dimensions into 2 dimensions while preserving the distances between shapes as far as possible. Labels "A" and "B" represent shapes at the 95% confidence boundary of a line drawn between the two mean shapes, which are represented as an open box (OA) and open circle (non-OA: control).

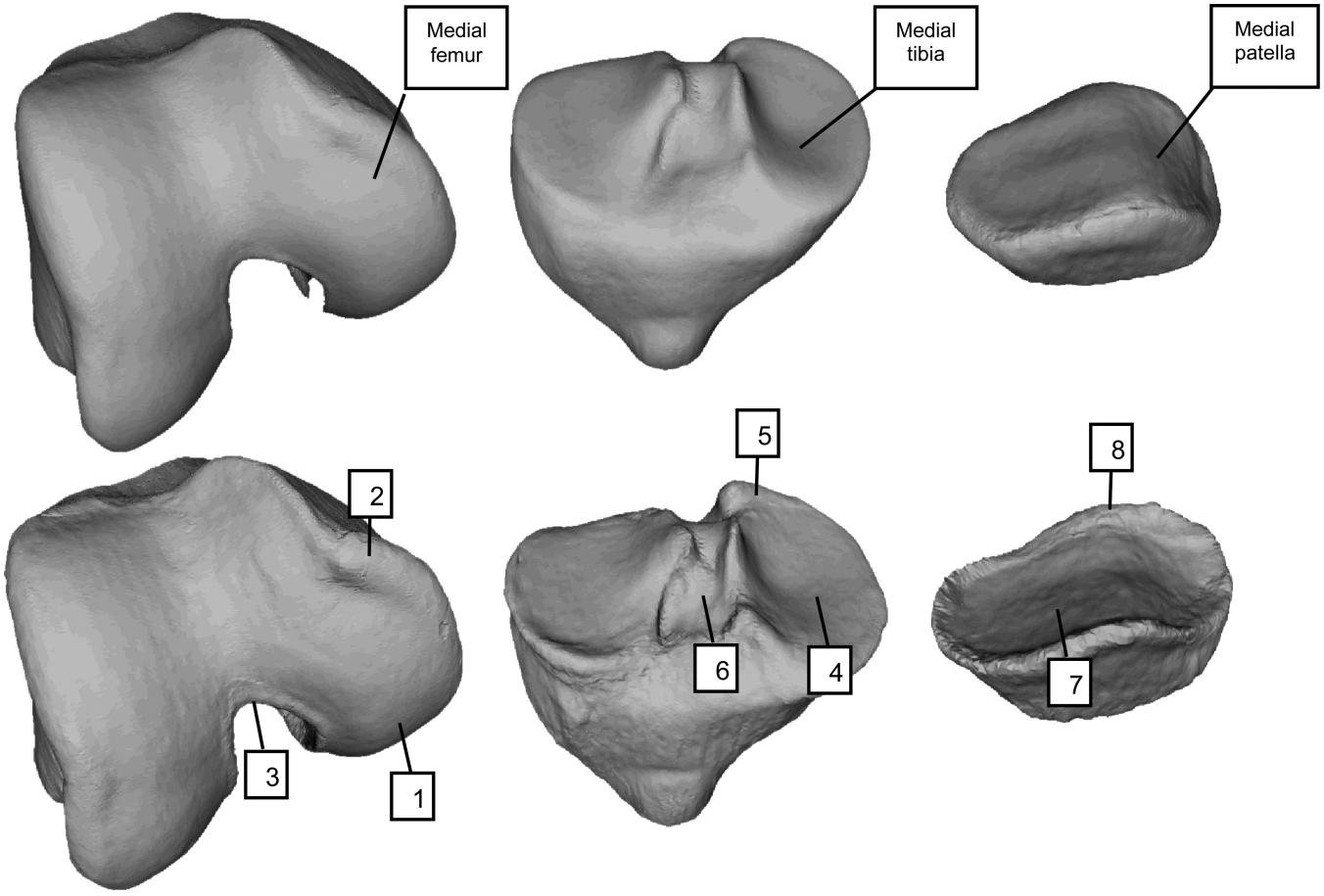

Figure 2.

Three-dimensional visualization of OA and control shapes (Labeled as “B” and “A”, respectively, in Figure 1). Top row depicts control shape for femur, tibia, and patella; bottom row depicts OA shape for those same bones. With OA, the femur shape changes include a widening and flattening of the condyles (1), increased ridge of osteophytic growth around the cartilage plate (2), and narrowing of the notch (3). Tibia shape changes include a widening and flattening of the condyles (4), increased ridge of osteophytic growth around the cartilage plate (5), and tibial spines moving closer together (6). The patella has similar patterns of increased size of the cartilage plate (7) and osteophytic ridge (8).

Table 1

Participant Characteristics

	Cases (N=178)	Controls (N=353)	P-value*
Mean age (SD)	61.3 (8.5)	61.2 (9.1)	0.8
Mean BMI (SD)	29.4 (4.5)	28.2 (4.5)	0.004
N (%) women	110 (61.8)	223 (63.2)	0.8
N (%) White	150 (84.3)	312 (88.3)	0.2
N (%) KL=0	46 (25.8)	92 (26.1)	1.0
KL=1	132 (74.2)	261 (73.9)	
Mean (SD) 3D bone shape vectors:			
Whole joint (femur, tibia, patella)			
Baseline	-0.32 (0.50)	-0.52 (0.53)	<0.0001
12-mo prior to incident OA	-0.23 (0.52)	-0.51 (0.54)	<0.0001
At incident OA	-0.01 (0.53)	-0.44 (0.57)	<0.0001
Tibiofemoral joint (femur, tibia)			
Baseline	-0.36 (0.55)	-0.54 (0.54)	0.0002
12-mo prior to incident OA	-0.27 (0.56)	-0.52 (0.57)	<0.0001
At incident OA	-0.04 (0.55)	-0.46 (0.59)	<0.0001
Femur only			
Baseline	-0.42 (0.62)	-0.63 (0.65)	0.0001
12-mo prior to incident OA	-0.33 (0.62)	-0.63 (0.67)	<0.0001
At incident OA	-0.10 (0.61)	-0.56 (0.70)	<0.0001
Tibia only			
Baseline	-0.40 (0.74)	-0.50 (0.69)	0.1
12-mo prior to incident OA	-0.28 (0.78)	-0.47 (0.72)	0.005
At incident OA	-0.04 (0.76)	-0.40 (0.74)	<0.0001
Patella only			
Baseline	-0.25 (0.96)	-0.51 (0.97)	0.003
12-mo prior to incident OA	-0.10 (1.00)	-0.46 (0.96)	<0.0001
At incident OA	+0.15 (1.06)	-0.37 (1.05)	<0.0001

*P-value for differences in means or proportions between cases and controls

Table 2

Relation of five 3D bone shape vectors 12 months prior to the index visit to risk of incident radiographic knee OA

3D bone shape vector*	%Case Knees with Incident Radiographic Knee OA	Crude OR	Adjusted† OR (95% CI)
Whole joint (femur, tibia, patella)			
Highest tertile	47	3.3	3.0 (1.8-5.0)
Middle tertile	31	1.6	1.5 (0.9-2.5)
Lowest tertile (ref)	22	1.0	1.0
P for linear trend:			p<0.0001
Per SD unit change towards OA	-	1.7	1.7 (1.4-2.1) p<0.0001
Tibiofemoral joint (femur, tibia)			
Highest tertile	43	2.8	2.5 (1.5-4.2)
Middle tertile	35	2.0	1.9 (1.1-3.1)
Lowest tertile (ref)	22	1.0	1.0
P for linear trend:			p=0.0004
Per SD unit change towards OA	-	1.6	1.5 (1.2-1.9) p<0.0001
Femur only			
Highest tertile	44	3.0	2.7 (1.7-4.5)
Middle tertile	36	2.1	2.0 (1.2-3.3)
Lowest tertile (ref)	21	1.0	1.0
P for linear trend:			p<0.0001
Per SD unit change towards OA	-	1.6	1.5 (1.3-1.9) p<0.0001
Tibia only			
Highest tertile	39	1.6	1.5 (0.9-2.4)
Middle tertile	32	1.1	1.1 (0.7-1.8)
Lowest tertile (ref)	29	1.0	1.0
P for linear trend:			p=0.08
Per SD unit change towards OA	-	1.3	1.3 (1.1-1.5) p=0.01
Patella only			
Highest tertile	47	2.4	2.2 (1.3-3.4)
Middle tertile	27	1.0	0.9 (0.6-1.4)
Lowest tertile (ref)	27	1.0	1.0
P for linear trend:			p=0.0009
Per SD unit change towards OA	-	1.5	1.4 (1.2-1.7) p=0.0005

*the vector range is -1 (mean non-OA shape) to +1 (mean OA shape); therefore lowest tertile is the referent group

†adjusted for age, sex, BMI

Table 3

Relation of five 3D bone shape vectors to risk of incident radiographic knee OA among knees that were KL=0 at baseline and in the whole sample concurrently at the time of incident OA

3D bone shape vector *	Adjusted† OR (95% CI)	
	Relation of 3D bone shape *12 months prior* to incident radiographic knee OA *among knees that were KL=0 at baseline*	**Relation of 3D bone shape *concurrently* with incident radiographic knee OA**
Whole joint (femur, tibia, patella)		
Highest tertile	12.5 (4.0-39.3)	9.6 (5.3-17.5)
Middle tertile	1.7 (0.6-5.2)	4.2 (2.4-7.6)
Lowest tertile	1.0 (ref)	1.0 (ref)
P for linear trend	p<0.0001	p<0.0001
Per SD unit towards OA	2.9 (1.7-4.7) p<0.0001	2.3 (1.8-2.9) p<0.0001
Tibiofemoral joint (femur, tibia)		
Highest tertile	7.1 (2.5-20.1)	6.4 (3.7-11.2)
Middle tertile	3.6 (1.3-9.6)	3.0 (1.7-5.3)
Lowest tertile	1.0 (ref)	1.0 (ref)
P for linear trend	p=0.0002	p<0.0001
Per SD unit towards OA	2.2 (1.4-3.5) p=0.0007	2.1 (1.7-2.7) p<0.0001
Femur only		
Highest tertile	6.5 (2.3-18.3)	6.5 (3.7-11.3)
Middle tertile	4.1 (1.5-11.1)	3.8 (2.2-6.5)
Lowest tertile	1.0 (ref)	1.0 (ref)
P for linear trend	p=0.0003	P<0.0001
Per SD unit towards OA	2.2 (1.4-3.5) p=0.0008	2.1 (1.7-2.6) p<0.0001
Tibia only		
Highest tertile	3.7 (1.4-9.7)	2.9 (1.8-4.7)
Middle tertile	3.5 (1.3-8.9)	1.7 (1.1-2.8)
Lowest tertile	1.0 (ref)	1.0 (ref)
P for linear trend	p=0.007	p<0.0001
Per SD unit towards OA	1.7 (1.1-2.6) p=0.01	1.6 (1.5-2.0) p<0.0001
Patella only		
Highest tertile	2.7 (1.0-7.1)	3.3 (2.0-5.4)
Middle tertile	1.0 (0.4-2.7)	1.8 (1.1-3.0)
Lowest tertile	1.0 (ref)	1.0 (ref)
P for linear trend	p=0.05	p<0.0001
Per SD unit towards OA	1.8 (1.1-2.7) p=0.01	1.6 (1.3-2.0) p<0.0001

*the vector range is -1 (mean non-OA shape) to +1 (mean OA shape); therefore lowest tertile is the referent group

†adjusted for age, sex, BMI

Table 4

Relation of five *baseline* 3D bone shape vectors to risk of incident radiographic knee OA in the whole sample and among knees that were KL=0 at baseline

3D bone shape vector tertiles*	Adjusted† OR (95% CI)			
	Relation of *baseline* 3D bone shape to incident radiographic OA *In the whole sample*		Relation of *baseline* 3D bone shape to incident radiographic OA *Among knees that were KL=0 at baseline*	
	Incident radiographic knee OA, *irrespective of time of OA onset*	Incident radiographic knee OA, *occurring 24-48 months later*	Incident radiographic knee OA, *irrespective of time of OA onset*	Incident radiographic knee OA, *occurring 24-48 months later*
Whole joint (femur, tibia, patella)				
Highest	2.5 (1.5-4.1)	3.0 (1.5-6.0)	6.2 (2.1-18.4)	6.6 (1.8-24.9)
Middle	1.8 (1.1-2.9)	2.6 (1.3-5.1)	2.0 (0.8-5.4)	2.2 (0.7-7.0)
Lowest	1.0 (ref)	1.0 (ref)	1.0 (ref)	1.0 (ref)
P for linear trend	p=0.0005	p=0.003	p=0.001	p=0.005
Per SD unit towards OA	1.5 (1.2-1.8) p=0.0003	1.6 (1.2-2.1) p=0.001	2.0 (1.3-3.1) p=0.0009	2.5 (1.4-4.6) p=0.002
Tibiofemoral joint (femur, tibia)				
Highest	1.8 (1.1-2.9)	2.4 (1.2-4.7)	4.2 (1.4-12.3)	6.0 (1.6-22.3)
Middle	1.6 (1.0-2.6)	2.3 (1.2-4.5)	2.8 (1.0-7.3)	3.1 (1.0-9.6)
Lowest	1.0 (ref)	1.0 (ref)	1.0 (ref)	1.0 (ref)
P for linear trend	p=0.03	p=0.01	p=0.008	p=0.006
Per SD unit towards OA	1.3 (1.1-1.6) p=0.003	1.5 (1.2-2.0) p=0.002	1.7 (1.2-2.5) p=0.004	2.4 (1.4-4.1) p=0.002
Femur only				
Highest	2.0 (1.2-3.3)	3.5 (1.7-6.9)	3.9 (1.4-10.5)	4.8 (1.5-15.6)
Middle	1.8 (1.1-2.9)	2.8 (1.4-5.5)	1.8 (0.7-4.7)	1.5 (0.5-4.8)
Lowest	1.0 (ref)	1.0 (ref)	1.0 (ref)	1.0
P for linear trend	p=0.006	p=0.0004	p=0.009	p=0.006
Per SD unit towards OA	1.4 (1.1-1.7) p=0.002	1.7 (1.3-2.3) p=0.0002	1.6 (1.1-2.3) p=0.007	2.2 (1.3-5.5) p=0.002
Tibia only				
Highest	1.2 (0.8-1.9)	1.4 (0.7-2.6)	2.6 (1.0-7.0)	2.3 (0.7-7.2)
Middle	1.0 (0.6-1.6)	1.3 (0.7-2.4)	1.0 (0.8-4.7)	1.9 (0.7-5.3)
Lowest	1.0 (ref)	1.0 (ref)	1.0 (ref)	1.0 (ref)
P for linear trend	p=0.4	p=0.3	p=0.04	p=0.1
Per SD unit towards OA	1.1 (0.9-1.4) p=0.2	1.2 (0.9-1.5) p=0.2	1.5 (1.0-2.3) p=0.06	1.5 (0.9-2.4) p=0.1
Patella only				
Highest	1.9 (1.1-3.0)	1.6 (0.8-3.2)	3.0 (1.1-8.3)	3.7 (1.0-14.0)
Middle	1.4 (0.9-2.3)	1.5 (0.8-2.8)	1.7 (0.7-4.2)	1.3 (0.4-4.0)
Lowest	1.0 (ref)	1.0 (ref)	1.0 (ref)	p=0.06
P for linear trend	p=0.01	p=0.2	p=0.04	

3D bone shape vector tertiles*	Adjusted† OR (95% CI)			
	Relation of ***baseline*** 3D bone shape to incident radiographic OA ***In the whole sample***		Relation of ***baseline*** 3D bone shape to incident radiographic OA ***Among knees that were KL=0 at baseline***	
	Incident radiographic knee OA, *irrespective of time of OA onset*	**Incident radiographic knee OA, *occurring 24-48 months later***	**Incident radiographic knee OA, *irrespective of time of OA onset***	**Incident radiographic knee OA, *occurring 24-48 months later***
Per SD unit towards OA	1.3 (1.1-1.6) p=0.01	1.2 (0.9-1.6) p=0.1	1.5 (1.0-2.2) p=0.07	1.5 (0.9-2.7) p=0.1

*the vector range is -1 (mean non-OA shape) to +1 (mean OA shape); therefore lowest tertile is the referent group

†adjusted for age, sex, BMI